Rare Met. (2018) 37(12):1064–1069
https://doi.org/10.1007/s12598-015-0666-3

RARE METALS
www.editorialmanager.com/rmet

Phase precipitation behavior and tensile property of a Ti–Al–Sn–Zr–Mo–Nb–W–Si titanium alloy

Wen-Jing Zhang, Xiao-Yun Song*, Song-Xiao Hui, Wen-Jun Ye, Wei-Qi Wang

Received: 7 November 2014 / Revised: 6 January 2015 / Accepted: 20 November 2015 / Published online: 19 December 2015

Abstract The characteristic of precipitation behavior of α_2 phase and silicide, and the tensile properties at room temperature and 650 °C after heat treatments in a novel Ti–Al–Sn–Zr–Mo–Nb–W–Si titanium alloy (BTi-6431S) were investigated by microstructure analysis and mechanics performance testing. The results show that no second phase precipitates after solution treatment (980 °C/2 h, air cooling (AC)). However, when the solution-treated specimens are aged at 600 °C (600 °C/2 h, AC), α_2 phase precipitates in the primary α phase, and the size of α_2 phase increases with the aging temperature increasing to 750 °C. Meanwhile, 50–100-nm S_2-type silicide particles precipitate along lamellar phase boundaries of transformed β phase after aging at 750 °C. BTi-6431S alloy shows the best 650 °C ultimate tensile strength (UTS) and yield strength (YS) when treated in solution treatment. However, aging treatment results in a decline in 650 °C ultimate tensile strength. This may be attributed to the loss of solution strengthening due to the depletion of Al, Si and Zr of the matrix caused by the precipitation of Ti_3Al and $(TiZr)_6Si_3$. Silicide is a brittle phase; therefore, its precipitation causes a sharp decrease in the room-temperature ductility of BTi-6431S alloy.

Keywords High-temperature titanium alloy; Precipitation behavior; α_2 phase; Silicide; Tensile properties

1 Introduction

Sky-rocketing development of high-speed vehicle has intensified the research on improving designs of hull materials. High-temperature titanium alloy with excellent properties, such as high specific strength and creep strength [1], is the right choice to be applied in high-speed vehicle. Concentrated efforts have resulted in the development of excellent titanium alloys to enhance the working temperature to about 600 °C, and typical examples are IMI834 [2], Ti-1100 [3] and Ti-600 [4]. These alloys belong to Ti–Al–Sn–Zr–Mo–Si titanium alloy which has less β-stabilizing elements. In order to further increase the service temperature, a new-type Ti–Al–Sn–Zr–Mo–Nb–W–Si titanium alloy, BTi-6431S alloy was designed through adding more Mo, Nb and W elements together to enhance β-phase strength, improving temperature capability and tensile situation up to 650–700 °C [5]. It has been found that the ultimate tensile strength (UTS) of this alloy at 650 °C can reach more than 600 MPa, which is almost equal to the UTS of Ti-1100 and BT36 at 600 °C (Ti-1100 is 630 MPa; BT36 is 640 MPa) [6]. Therefore, BTi-6431S alloy is expected to be used for short-time structural components at 650–700 °C in aerospace industry.

Since high-temperature titanium alloys typically contain 4 wt%–8 wt% aluminum, aging may result in the formation of the ordered and coherent precipitation, α_2 phase (Ti_3Al)

W.-J. Zhang, X.-Y. Song*, S.-X. Hui, W.-J. Ye
State Key Laboratory for Fabrication and Processing of Nonferrous Metals, General Research Institute for Nonferrous Metals, Beijing 100088, China
e-mail: songxiaoyun82@126.com

W.-J. Zhang
School of Materials and Metallurgy, Northeastern University, Shenyang 110819, China

W.-Q. Wang
Baoti Group Co., Ltd., Baoji 721014, China

[7]. Madsen and Ghonem [8] investigated that the precipitation of α_2 phase after aging in Ti-1100 alloy was largely responsible for the increase in the yield strength (YS) at 593 °C and decrease in ductility at room temperature (RT). In many titanium alloys, silicon is added as a solid solution strengthener to improve high temperature strength and creep resistance. Aging may also promotes the formation of silicide in the silicon-bearing titanium alloys. Two kinds of silicide were reported in earlier studies that is S_1 ($(TiZr)_5Si_3$) and S_2 ($(TiZr)_6Si_3$). Both of them are hexagonal but with different lattice parameters (for S_1, $a \approx 0.78$ nm, $c \approx 0.54$ nm; for S_2, $a \approx 0.70$ nm, $c \approx 0.36$ nm). The precipitation of different types of silicide depends on the composition and heat treatment. Usually, silicide is a brittle phase, and its precipitation causes a big loss in ductility [9, 10].

In this work, BTi-6431S alloy contains relatively high Al content and 0.2 wt% Si, so aging may produce α_2 phase and silicide in this alloy. Previous work mainly deals with the role of α_2 phase and silicide on tensile properties of other titanium alloys under 600 °C [11]. Thus, few data exist on mechanical properties over 600 °C. The present investigation aims to study the precipitation behavior of α_2 phase and silicide in BTi-6431S alloy after different heat treatments, and the effects of second phases on RT and 650 °C tensile properties.

2 Experimental

The composition of BTi-6431S alloy used in this research contains 6.21 wt% Al, 3.15 wt% Sn, 2.86 wt% Zr, 1.19 wt% Mo, 1.12 wt% Nb, 0.45 wt% W and 0.20 wt% Si. The ingot was melted three times by the vacuum consumable electrode method, then forged and hot-rolled in ($\alpha + \beta$) two-phase region to a 3-mm-thickness plate. The β-transus temperature of this alloy was 990–1000 °C measured by metallographic techniques. The microstructure of as-received material is composed of lath-shaped primary α phase (α_p) and lamellar transformed β phase (β_t), as shown in Fig. 1.

Three kinds of heat treatments, as designated in Table 1, were conducted on BTi-6431S plates using a resistance heating furnace. The tensile specimens with dimensions of 3 mm × 15 mm and a gage length of 50 mm were cut from the heat-treated plates along the rolling direction. RT and 650 °C tensile tests were conducted on an Instron 5582 testing machine at a strain rate of 0.04 and 0.005 min^{-1}, respectively. At least three specimens were tested for each treatment to make an average. Microstructures were observed by Axiovert 200 MAT Zeiss metallographic microscope (OM) and JEM2100 transmission electron microscope (TEM). Tensile fracture surface was observed by JSM-7001 scanning electron microscope (SEM). Compositions of each phase were measured on JXA-8100 electron probe microanalyzer (EPMA). Specimens for OM were prepared by conventional mechanical polishing techniques and etched with a solution of 10 ml HF, 30 ml HNO_3 and 70 ml H_2O. The foils for TEM observations were prepared by twin-jet polishing technique using a solution of 70 vol% methanol, 21 vol% butanol and 9 vol% perchloric acid, at a current of 55–60 mA and a temperature from −20 to −30 °C.

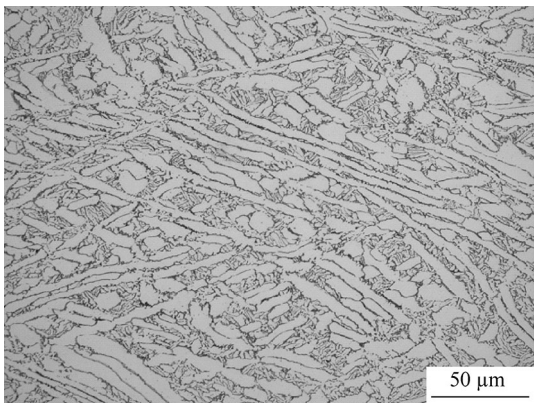

Fig. 1 OM image of original material

Table 1 Heat treatments of BTi-6431S alloy

Process	Solution treatment	Aging treatment
ST	980 °C/2 h, AC	None
STA1	980 °C/1 h, AC	600 °C/2 h, AC
STA2	980 °C/1 h, AC	750 °C/2 h, AC

3 Results and discussion

3.1 Observation of microstructure

Figure 2 shows the microstructure of the alloys after different heat treatments. All the three specimens consist of bimodal microstructures, i.e., α_p and β_t. However, aging treatment changes the content of α_p. The content of α_p in the solution-treated (ST) specimen is about 40 vol% and increases to 42 vol% by the following aging at 600 °C. With the aging temperature increasing, the content of α_p in the STA2 condition further increases to 50 vol%.

The concentration of each element in α_p and β_t after different heat treatments is listed in Table 2. α_p has more Al than β_t, the content of Al in α_p and β_t decreases after follow-up aging treatment, and the decrement gets larger

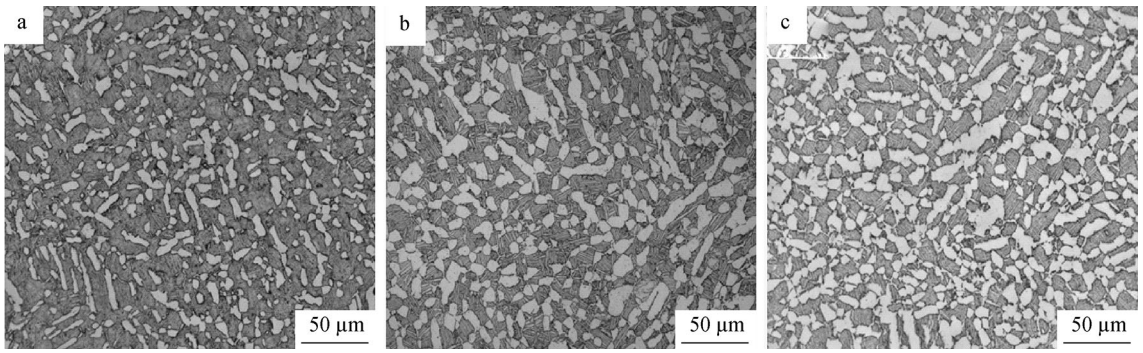

Fig. 2 OM images of samples after different heat treatments: **a** ST, **b** STA1 and **c** STA2

Table 2 Composition of each phase after different heat treatments by EPMA (wt%)

Process	Phases	Al	Sn	Zr	Mo	Nb	W	Si
ST	α_p	7.284	2.790	2.439	0.287	0.596	0.058	0.106
	β_t	5.621	3.229	2.927	1.617	1.289	0.513	0.159
STA1	α_p	7.171	2.717	2.211	0.230	0.546	0.012	0.128
	β_t	5.349	3.478	3.22	1.775	1.322	0.578	0.149
STA2	α_p	6.434	2.952	2.477	0.581	0.905	0.049	0.128
	β_t	5.173	3.298	2.39	2.310	1.566	0.648	0.095

with the aging temperature increasing. As β stabilizers, Mo, Nb and W mainly exist in β_t [12], and their contents increase with aging temperature rising.

3.2 Precipitation characteristics of second phase

The precipitation features of second phases after different heat treatments were investigated by TEM. In ST condition, no second-phase particles are observed. After aging treatments, the selected area electron diffraction (SAED) pattern and corresponding dark field image (DFI) of α_p are shown in Fig. 3, indicating that large quantities of coherent and ordered α_2-phase particles precipitate in α_p. With the aging temperature increasing from 600 to 750 °C, the size of α_2-phase particle grows from 5 to 10 nm, as shown in Fig. 3b, d.

Figure 4 exhibits the TEM images of β_t in STA1 and STA2 conditions. It can be found that no second phase precipitates in β_t of STA1 sample, as shown in Fig. 4a. However, elliptical second-phase particles with size of 50–100 nm precipitate along the lamellar phase boundaries in STA2 specimen, as indicated by the arrows in Fig. 4b. From the corresponding SAED pattern in Fig. 4b, this phase is indexed as hexagonal S_2-type silicide with $[12\bar{1}6]$, $a = 0.698$ nm and $c = 0.367$ nm. This is well consistent with the results of IMI829, IMI834 and BT9 alloys, as reported by Singh et al. [13]. The composition of this phase was measured by TEM equipped with energy-dispersive spectroscopy (EDS) as 33Si–35Zr–32Ti (at%), which is also in accordance with $(TiZr)_6Si_3$ (S_2-type silicide).

3.3 Tensile property

Figure 5 summarizes the tensile properties, including YS, UTS and elongation (EL), at RT and 650 °C of BTi-6431S alloy after different heat treatments. Compared with ST specimen, the RT tensile properties of the STA1 specimen almost remain constant, whereas the value of EL for STA2 specimen decreases dramatically from 8.0 % to 2.5 %. On the contrary, the YS and UTS at 650 °C drop gradually after aging at 600 and 750 °C, while the EL of all specimens at 650 °C is more than 20 %. At 650 °C, the values of YS and UTS are 400 and 605 MPa for ST specimen and 350 and 545 MPa for STA2 specimen, respectively. The results indicate that aging treatment greatly affects the RT ductility and 650 °C tensile strength.

3.4 Precipitation behavior of second phase

In the present investigation, aging at 600 and 750 °C for 2 h results in the precipitation of ordered α_2 phase, and the size of α_2 phase gets larger when aging at higher temperature. It is reported that the precipitation of α_2 phase is accompanied with element diffusion [14]. Therefore, increasing aging temperature could raise the diffusion rate of atoms, accelerate the growth and finally coarsen α_2-phase particles.

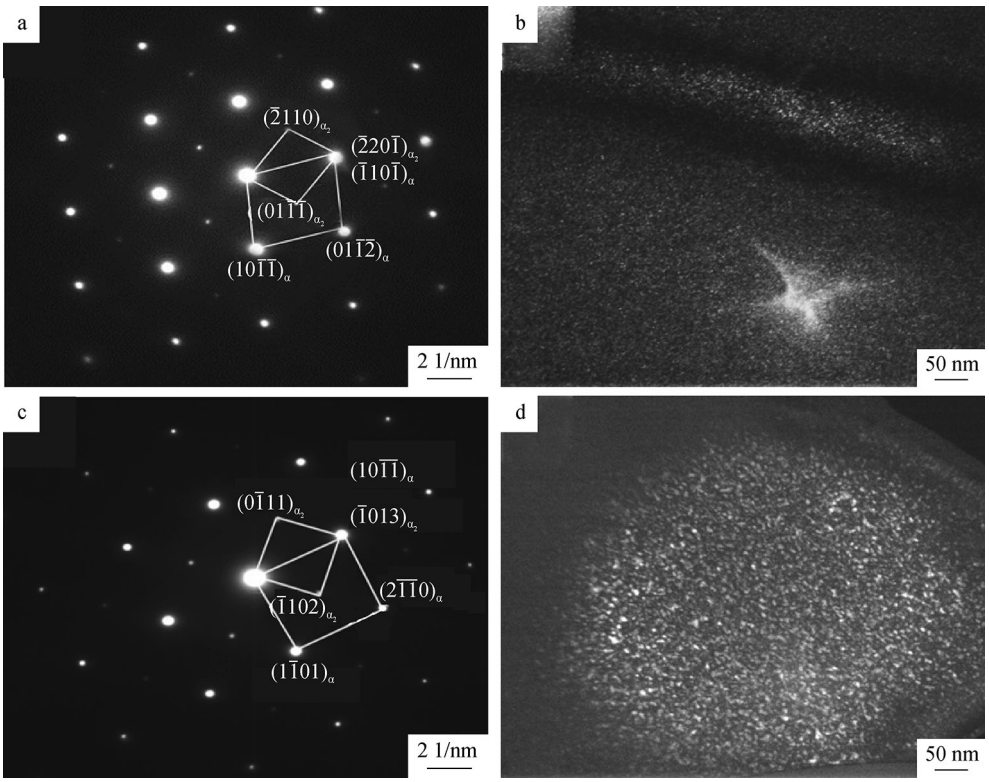

Fig. 3 TEM images of BTi-6431S alloy: **a** SAED pattern of α_p with $[01\bar{1}1]_{\alpha}\|[01\bar{1}2]_{\alpha_2}$ in STA1 condition, **b** DFI of α_p in STA1 condition, **c** SAED pattern of α_p with $[01\bar{1}1]_{\alpha}\|[5\bar{1}\bar{4}3]_{\alpha_2}$ in STA2 condition and **d** DFI of α_p in STA2 condition

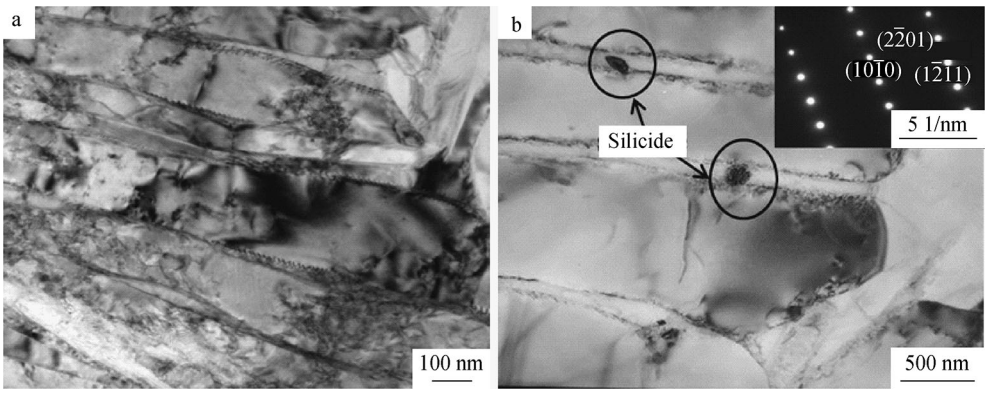

Fig. 4 TEM images of β_t in different conditions: **a** STA1 and **b** STA2

On the other hand, aging at 750 °C for 2 h results in the precipitation of silicide particles, while aging at lower temperature (600 °C) for the same time could not. This could be understood in terms of the relative increase in the amounts of the β-stabilizing elements in the reduced content of β_t with the increase in the aging temperature, which finally accelerates such precipitation [10, 11]. From the EPMA result in Table 2, it can be inferred that β_t has the highest content of β stabilizers after aging at 750 °C. The role of the higher β stabilizers in enhancing the kinetics of precipitation of silicide has been brought out recently [15]. In this alloy, only the S_2-type silicide precipitates predominantly along the lamellar phase boundaries in β_t under the aging condition. This phenomenon is in agreement with the observation in IMI829 and BT9 alloys [13, 16].

3.5 Influence of second phases on tensile properties

For titanium alloys, many investigations reported that the precipitations of ordered α_2 phase and silicide produce

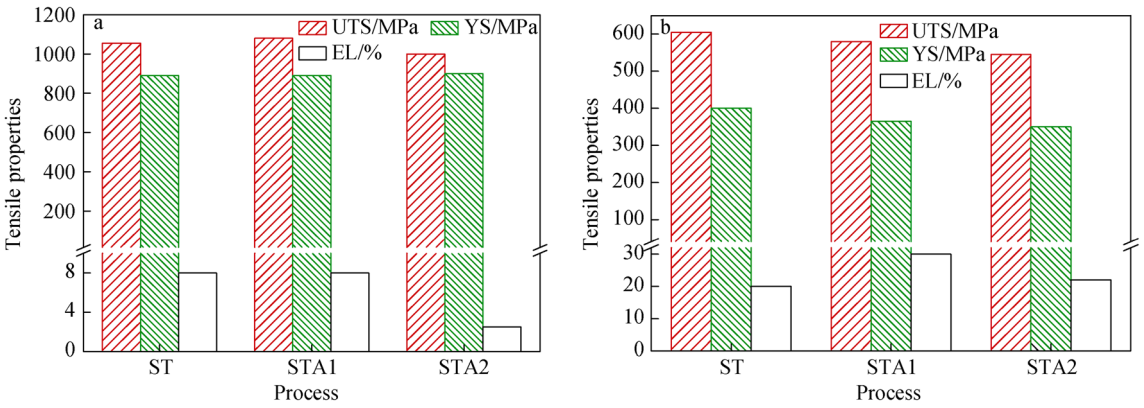

Fig. 5 Tensile properties at different temperatures after each heat treatment: **a** RT and **b** 650 °C

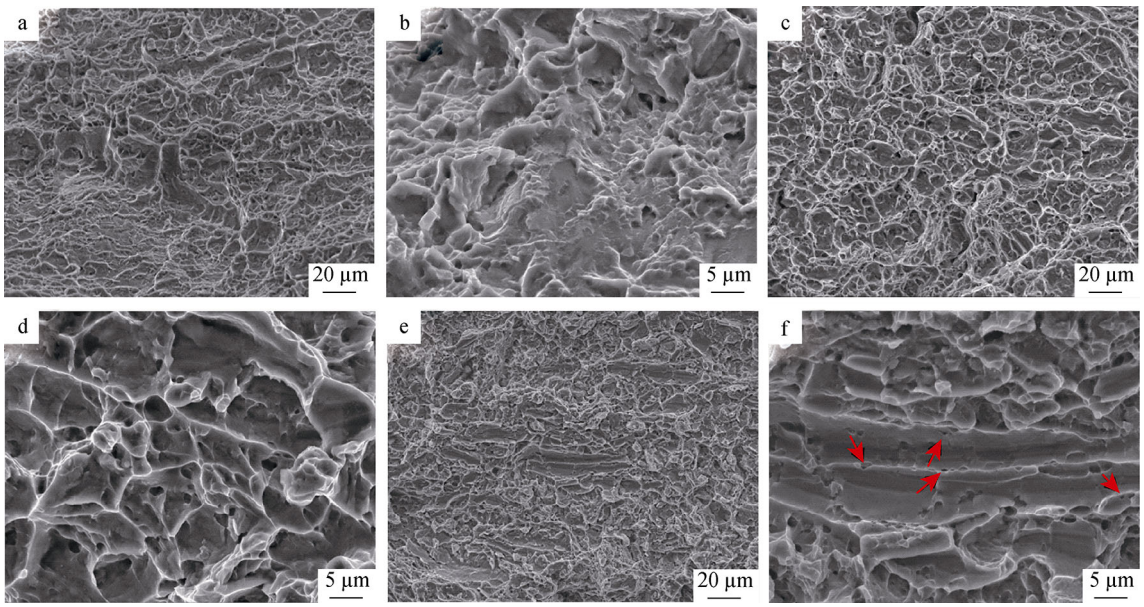

Fig. 6 SEM images of tensile fractographs at RT of BTi-6431S alloy with different heat treatments: **a**, **b** ST; **c**, **d** STA1; **e**, **f** STA2

dispersion strengthening effect; however, their precipitation could weaken solid solution strengthening effect and RT ductility. So the strengthening effect is a balance between increasing and decreasing due to the second-phase precipitation when solution elements are taken out of solution.

In BTi-6431S alloy, α_2-phase precipitation in STA1 specimen does not affect RT strength and ductility. However, the RT ductility of STA2 specimen with S_2-type silicide is lower than those of ST and STA1 specimens. This is obviously due to the detrimental role of the precipitation of brittle silicide. Ramachandra et al. [17] also found the same phenomenon in oil-quenched IMI685 alloy aged at 800 °C (only S_2-type silicide formed). The fractographs in Fig. 6 bring out the distinct differences in the fracture behavior of the different specimens after tensile tests. The fracture surfaces of ST and STA1 specimens contain dimples and fracture facets with tearing ridge surrounded, as shown in Fig. 6a–d, indicating a mixture mode of ductile fracture and transgranular cleavage fracture. However, the fracture surface of STA2 specimen is covered with fracture facets, as shown in Fig. 6e, suggesting that quasi-cleavage fracture is the primary fracture mode. Amplifying the fractographs of specimen treated in STA2 condition, there are small voids distributed randomly along the lamellar phase boundaries in β_t, as indicated by the arrows in Fig. 6f. Ramachandra et al. [17] reported that the tendency for faceted fracture is significantly enhanced due to the silicide precipitation in β_t. So the silicide precipitation in STA2 specimen promotes voids initiation, resulting in the cleavage facets in β_t.

The 650 °C tensile strength decreases after aging treatment, especially in STA2 condition. It proves that at 650 °C, the ineffective role of the second phases on strengthening is coined with the decrease in solid solution strengthening due to the depletion of Al, Si and Zr which are the main elements composing Ti_3Al and $(TiZr)_6Si_3$. As shown in Table 2, STA2 specimen has the least contents of Al in α_p and Si and Zr in β_t.

High-temperature tests do not show the trend toward reduced ductility after aging treatment. However, in contrast to RT results, the difference in ductility between unaged and aged specimens is much less pronounced. It could be concluded that the silicide precipitation does not damage 650 °C ductility in BTi-6431S alloy. For BTi-6431S alloy, in order to guarantee the RT ductility and 650 °C strength, the single solution treatment is appropriate.

4 Conclusion

BTi-6431S alloy was heat-treated by solution and aging treatments. Aging causes the formation of two types of precipitates, α_2 phase and S_2-type silicide. The precipitation behavior and the effects of them on tensile properties at room temperature and 650 °C were studied. In BTi-6431S alloy, large quantities of 5-nm-ordered α_2 particles precipitate within α_p after aging at 600 °C for 2 h, and their sizes increase to about 10 nm when aging temperature rises to 750 °C. After aging at 750 °C, due to the higher content of β stabilizer in β_t, some S_2-type silicide $(TiZr)_6Si_3$ particles with size of 100 nm precipitate along the lamellar phase boundaries in β_t. Compared with the solution-treated and 600 °C aged alloys, the RT ductility of the alloy aged at 750 °C decreases dramatically, because of the precipitation of incoherent brittle silicide. After aging at 600 and 750 °C, although Ti_3Al and $(TiZr)_6Si_3$ could produce precipitation strengthening effect, their precipitation also results in the decrease in Al, Si and Zr contents dissolved in matrix, leading to the loss of solid solution strengthening effect. Consequently, the tensile strength at 650 °C decreases gradually.

Acknowledgments This work was financially supported by the National Natural Science Foundation of China (No. 51201016).

References

[1] Boyer RR. An overview on the use of titanium in the aerospace industry. Mater Sci Eng A. 1996;213(1–2):103.
[2] Wanjara P, Jahazi M, Monajati H, Yue S, Immarigeon JP. Hot working behavior of a near-α alloy IMI834. Mater Sci Eng A. 2005;396(1–2):50.
[3] Chandravanshi VK, Sarkar R, Kamat SV, Nandy TK. Effect of boron on microstructure and mechanical properties of thermo-mechanically processed near alpha titanium alloy Ti-1100. J Alloys Compd. 2011;509(18):5506.
[4] Zhao JW, Ding H, Hou HL, Li ZQ. Influence of hydrogen content on hot deformation behavior and microstructural evolution of Ti600 alloy. J Alloys Compd. 2010;491(1–2):673.
[5] Zhang WJ, Song XY, Hui SX, Ye WJ, Wang YL, Wang WQ. Tensile behavior at 700 °C in Ti–Al–Sn–Zr–Mo–Nb–W–Si alloy with bi-modal microstructure. Mater Sci Eng A. 2014;595:159.
[6] Zhang WJ, Song XY, Hui SX, Ye WJ, Wang YL, Wang XX. Effect of single annealing on the microstructure and mechanical properties of BTi-6431S titanium alloy. Chin J Nonferrous Met. 2013;23(6):1530.
[7] Woodfield AP, Postans PJ, Loretto MH, Smallman RE. The effect of long-term high temperature exposure on the structure and properties of the titanium alloy Ti5331S. Acta Metall. 1998;36(3):507.
[8] Madsen A, Ghonem H. Separating the effect of Ti_3Al and silicide precipitates on the tensile and crack growth behavior at room temperature and 593 °C in a near-α titanium alloy. Mater Eng Perform. 1995;4(3):301.
[9] Srinadh KVS, Singh N, Singh V. Role of Ti_3Al/silicide on tensile properties of Timetal 834 at various temperatures. Bull Mater Sci. 2007;30(6):595.
[10] Madsen A, Audrieu E, Ghonem H. Microstructural changes during aging of a near-α titanium alloy. Mater Sci Eng A. 1993;171(1–2):191.
[11] Gogia AK. High-temperature titanium alloy. Def Sci J. 2005;55(2):149.
[12] Leyans C, Peters M. Titanium and Titanium Alloys. Weinheim: Wiley-VCH Verg Gmbh & Co. KGaA; 2003. 11.
[13] Singh AK, Ramachandra C, Tavafoghi M, Singh V. Microstructure of β-solution-treated, quenched and aged α + β titanium alloy Ti–6Al–1.6Zr–3.30Mo–0.3Si. J Alloys Compd. 1992;179(1–2):125.
[14] Zhang J, Wang QJ, Liu YY, Li L, Li D. Optimal selection and control for precipitation of α_2 phase in near α high temperature Ti alloy during aging treatment. J Mater Sci Technol. 2004;20(5):574.
[15] Ramachandra C, Singh AK, Sarma GMK. Microstructure characterization of near-α titanium alloy Ti–6Al–4Sn–4Zr–0.70Nb–0.50Mo–0.40Si. Metall Trans A. 1993;24(6):1273.
[16] Sridhar G, Sarma DS. Structure and properties of a β solution treated, quenched, and aged Si-bearing near-α titanium alloy. Metall Trans A. 1989;20(1):55.
[17] Ramachandra C, Singh V. Effect of silicide precipitation on tensile properties and fracture of alloy Ti–6Al–5Zr–0.5Mo–0.25S. Metall Trans A. 1985;16(2):227.